

## Relaxing in foam

A D . Gopal and D J. Durian

UCLA Department of Physics & Astronomy, Los Angeles, CA 90095-1547  
(Dated: May 21, 2019)

We investigate the mechanical response of an aqueous foam, and its relation to the microscopic rearrangement dynamics of the bubble-packing structure. At rest, even though the foam is coarsening, the rheology is demonstrated to be linear. Under flow, shear-induced rearrangements compete with coarsening-induced rearrangements. The macroscopic consequences are captured by a novel rheological method in which a step-strain is superposed on an otherwise steady flow.

PACS numbers: 82.70.Rr, 83.60.Rs, 83.80.Lz, 83.85.Cg

Aqueous foams are tightly packed collections of gas bubbles separated by a continuous liquid phase [1, 2]. Like elastic solids, bulk foams resist shear, completely unlike the gases and liquids from which they are comprised. The origin of this striking behavior is that the bubbles are jammed, unable to flow around one another and explore conformational space under thermal energy. Thus bubbles distort, rather than rearrange, when subjected to small shear deformations. The resulting extra internal gas-liquid surface area costs energy in proportion to the surface tension, and this provides a restoring force. The order of magnitude of the static shear modulus is simply surface tension divided by bubble radius. The precise value depends on the volume fraction,  $\phi$ , of the liquid phase [3, 4, 5]. As a foam is made wetter, the bubbles become progressively rounder, and the shear modulus decreases. The elasticity completely vanishes at the point where the bubbles are close-packed spheres. This is one example of an unjamming transition [6].

In this paper we explore alternative ways to unjam the bubbles in a foam. Each could correspond to a different trajectory in a global jamming phase diagram [7]. For example, one could imagine raising the temperature so that  $k_B T$  is greater than  $R^2$ , which would allow the bubbles to rearrange themself like Brownian particles. However, a typical value is  $R^2 = k_B^{-1} 10^{12} \text{ K}$ ; therefore, foams are athermal far-from-equilibrium systems and raising the temperature is not feasible. But there are at least two other ways to drive the system so that bubble rearrangements occur. One is through coarsening, the diffusion of gas from smaller to larger bubbles. As this proceeds, local stress inhomogeneities repeatedly build up to some threshold and relax by sudden avalanche-like local rearrangements. Such microscopic dynamics have been observed previously via diffusing-wave spectroscopy (DWS) [8, 9, 10]. This raises a string of interesting questions. How do localized coarsening-induced rearrangements affect the linear shear rheology of bulk foams? Is the effect similar to thermally excited dynamic heterogeneities in glassy systems? A second, entirely different, way to induce rearrangements is by shearing the sample. Here local stresses also accrue and relax, but in a more correlated manner. These rearrangement dynamics have similarly

been studied by DWS [11, 12, 13]. How does the elastic character of foam vanish as the shear rate is increased? Can we think of the two driving mechanisms as "heating" and ultimately unjamming the sample? To make progress, here we study the mechanical response of a single aqueous foam, at very long times / low frequencies and, in a novel twist, as a function of shear rate.

All measurements were made on a commercial aqueous foam, consisting of nearly-spherical polydisperse gas bubbles, 92% by volume, that are tightly packed in an aqueous solution of stearic acid and triethanolamine (Gillette Company, Boston MA). Samples are surrounded by a water bath held at 25.0 C and are measured after the foam has aged for approximately 100 minutes. By this time, the average bubble size is approximately 60 microns and is growing reproducibly via coarsening [20]; stresses due to the loading process have also relaxed. Test durations are sufficiently short that gravitational liquid drainage and bubble coalescence are negligible.

All measurements were performed with a Paar Physica UDS 200 rheometer, controlling the rotational speed and angular displacement of a solid cylinder whose axis is vertical and concentric with a fixed surrounding cup. The sample cell has an inner radius of 20.0 mm, and a 4.1 mm gap; these dimensions ensure that the foam can be treated as a bulk material with uniform stress. To minimize end-effects, the 98 mm long inner cylinder is much shorter than the depth of the surrounding cup yet much longer than the gap width. Wall slip is precluded by coating both the cylinder and cup with a fine-grade sandpaper. Samples are loaded through a 5 mm hole at the bottom of the cup, after lowering the cylinder to the test position. DWS measurements indicate the absence of shear-banding and other secondary flows [13]. To reconfirm, we compared with a similarly coated cone-and-plate cell, with a 10 cm radius and 10 cone angle. Identical rheology results were obtained for both cell configurations, implying that the imposed shear deformation is uniform.

Effect of coarsening on mechanical response. The standard measure of linear response is the frequency-dependent complex shear modulus,  $G^*(\omega) = G'(\omega) + iG''(\omega)$ , defined by the ratio of oscillatory stress to os-

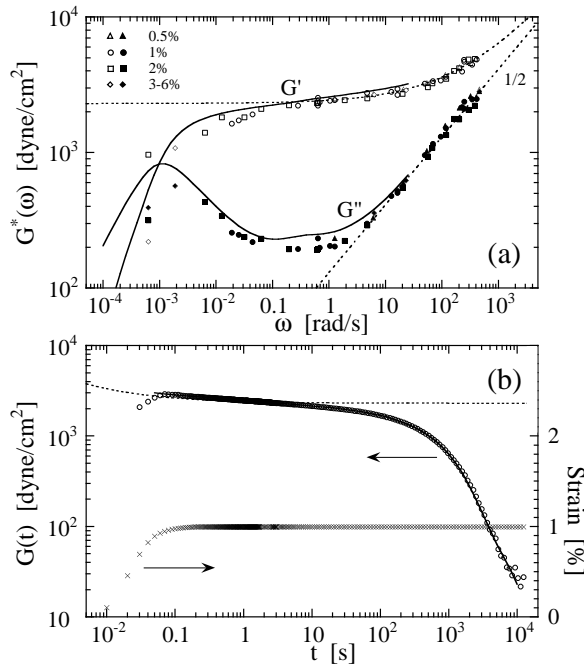


FIG. 1: Dynamic shear moduli of a coarsening foam, in both the (a) frequency and (b) time domains. The dashed curves in (a-b) are a fit to  $G^*(\omega) = G_0(1 + i\omega\tau_c)$  and  $G(t) = G_0(1 + 1 - e^{-t/\tau_c})$ , predicted for nonaffine bubble motion in the absence of any time evolution. The solid curve in (b) is an empirical fit to  $G(t)$ ; appropriately transformed, it gives the solid curves matching the storage and loss moduli in (a).

cillatory strain [14, 15]. The in- and  $\pi/2$  out-of-phase components,  $G'(\omega)$  and  $G''(\omega)$ , respectively represent the purely elastic and dissipative parts of the response. Data for a coarsening, unsheared, foam are shown in Fig. 1. We observe that  $G'(\omega)$  is larger than  $G''(\omega)$  for nearly six decades in frequency, consistent with the notion that foams are primarily elastic. A crucial point is that these results are indistinguishable for the four different applied strain amplitudes, which is a minimal requirement for linear response. Note that the difference between  $G'(\omega)$  and  $G''(\omega)$  is greatest (i.e. the foam is most elastic), and the respective values are nearly frequency-independent, in the middle of the frequency range. Early measurements [4, 16, 17] were restricted to this regime, which caused a puzzle regarding the low-frequency behavior where on general grounds one expects  $G''(\omega) \gg G'(\omega)$  [18]. Our data extend the observed spectrum considerably, enough to resolve this puzzle as will be seen.

The form of  $G^*(\omega)$  observed in Fig. 1(a) is certainly not consistent with foam being a so-called Kelvin solid, where  $G^*(\omega) = G + i\omega\eta$ . Rather, the behavior for  $\omega > 5$  rad/s is more like  $G^*(\omega) = G_0(1 + i\omega\tau_c)$ . The dotted curves in Fig. 1(a) are fits to this form, with  $G_0 = 2300$  dyne/cm<sup>2</sup> and  $\tau_c = 156$  rad/s. The former represents the shear modulus. The latter represents the consequence of nonaffine deformation of the bubbles

under shear due to local packing configurations that are weak/strong with respect to the shear direction [19]. This was seen previously in  $G''(\omega)$  for a foam [17], but the frequencies were too low to observe the required contribution to  $G''(\omega)$ . Deviations from the fit that set in below about 5 rad/s indicate the effects of coarsening.

To investigate low frequency behavior, and the role of coarsening, it is preferable to work in the time domain (our lowest frequency already corresponds to 2 divided by sample age). Thus we measure the shear stress relaxation modulus,  $G(t)$ , defined by the ratio of the time-dependent stress following the imposition of an instantaneous step-strain. Our results are shown in Fig. 1(b), along with the actually-imposed strain (which has a rise time of about 0.05 s). The dotted curve represents  $G(t) = G_0(1 + 1 - e^{-t/\tau_c})$ , the transform of the high-frequency fit to  $G^*(\omega)$ . It is consistent with the data for times shorter than about 5 s; this is a very stringent test of linear response. At longer times, the stress decays slowly, almost logarithmically, over a few decades in time before relaxing more rapidly beyond about 1000 s. According to DWS, coarsening-induced rearrangements occur every  $\tau_q = 20$  s at each scattering site. This corresponds to roughly the onset of deviation from the high-frequency behavior, but not to the stress relaxation time. This implies that individual rearrangements are relatively ineffective in relaxing globally-imposed stress. Rather, the stress relaxation time is set by the age of the sample. Since the average bubble size grows as a power law [20], this is the time required for an appreciable change in bubble size. The cumulative effect of many rearrangements at each site is required for stress relaxation. The resulting functional form for  $G(t)$  seen in Fig. 1(b) is not well understood. The solid curve is an empirical fit to a sum of exponentials (Maxwell modes). The corresponding transform of this fit is also shown in Fig. 1(a). It agrees very well with the low-frequency behavior of the  $G^*(\omega)$  data. Thus linear response holds. This is remarkable, given that the microscopic relaxation mechanism isn't thermal, but rather an evolution mechanism. Here, evolution causes complete stress relaxation, so that at long times the foam is unjammed and behaves like an equilibrium liquid.

Effect of shear on mechanical response. Next we investigate how the application of shear causes a similar loss of elasticity. For this we superimpose a small-amplitude step-strain,  $\gamma_0$ , on top of otherwise steady shear at rate  $\dot{\gamma}$ . The resulting temporary increase in stress defines the transient stress relaxation modulus,  $G(t; \dot{\gamma}) = [G(t) - G(0; \dot{\gamma})] / \gamma_0$ . A frequency-domain version of this technique was developed for polymers [21]. Example data are shown in Fig. 2(a). Note that as the strain rate increases, the elastic character of the foam melts away. There are two signs of this. First, the progressively smaller intercept,  $G(0; \dot{\gamma})$ , means less elastic energy storage. Second, the progressively shorter decay

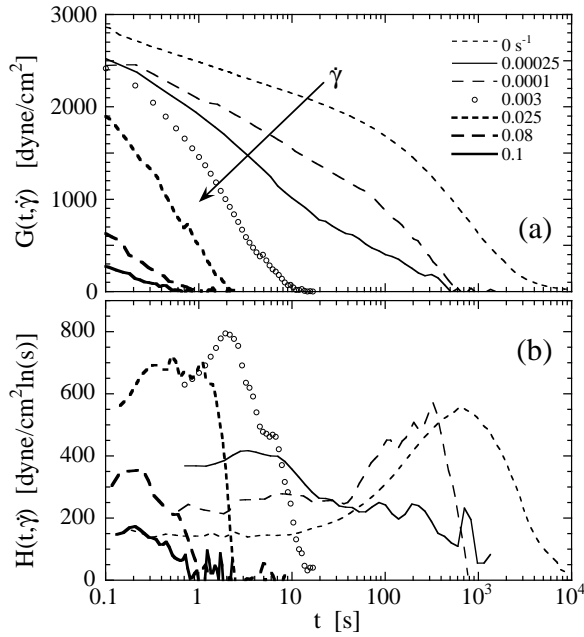


FIG. 2: (a) Stress relaxation moduli for foams sheared at various rates, as listed. This is given from the stress  $\sigma(t)$  following the superposition of a step-strain on steady shear:  $G(t; \dot{\gamma}) = [\sigma(t) - \sigma(0)] / \dot{\gamma}$ . (b) The corresponding relaxation spectra, given by differentiating vs the logarithm of time.

time means more liquid-like dissipation. At high enough strain rates, where there is no transient storage and only dissipation, the foam behaves like an equilibrium liquid. Similar behavior has now been observed in simulations of a model foam [22].

To further quantify the unjamming behavior apparent in Fig. 2 (a), we first deduce the relaxation spectrum,  $H(t; \dot{\gamma})$ , defined by  $G(t; \dot{\gamma}) = \int_0^t H(\tau; \dot{\gamma}) \exp(-t/\tau) d \ln \tau$ . Results are shown in Fig. 2 (b). For low and zero strain rates, there are two competing relaxation processes, reflected by a broad peak at very late times and long tail of short-time modes of nearly equal weight. The former reflects the coarsening process, and the latter the non-affine bubble motion. As the shear rate increases, the coarsening peak gradually falls and another peak gradually rises over the non-affine tail at short times. Presumably this is due to shear-induced rearrangements.

The salient features of the stress relaxation are shown in Fig. 3 vs strain rate. The first plot is of elastic storage,  $G(0; \dot{\gamma})$ , the value when the superimposed step-strain is achieved (below about 0.1s). This decreases very slowly, and is nearly constant, for strain rates less than about 0.05/s; for higher strain rates it abruptly vanishes. The second plot is of stress relaxation times. One such measure is  $t_e$ , when stress falls to 1/e of the initial value. Another measure is  $t_p$ , when the relaxation spectrum reaches its peak. At zero and very low strain rates, these times are different since there are two competing relaxation mechanisms (evolution and shear). For strain rates

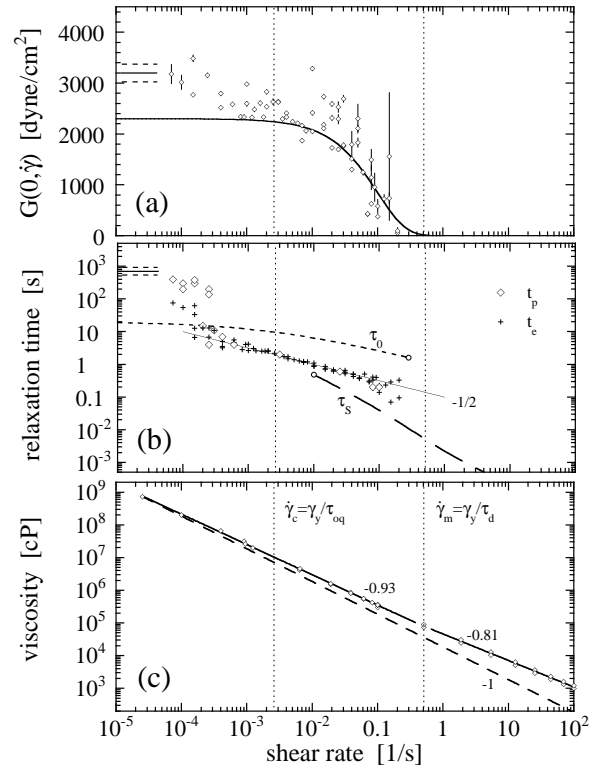


FIG. 3: (a) Transient shear modulus, (b) transient shear relaxation times, and (c) viscosity, all as a function of shear rate. The vertical dotted lines denote the characteristic shear rates set by the yield strain divided respectively by the time between rearrangements and the duration of rearrangements in a quiescent foam. In (a), the solid curve is  $G_0 \exp[-(\dot{\gamma}/0.1 \text{ s}^{-1})]$  where  $G_0 = 2300$  dyne/cm<sup>2</sup> is the shear modulus. In (b), the open diamonds indicate where  $H(t; \dot{\gamma})$  is a maximum and pluses indicate where  $G(t; \dot{\gamma})$  falls to 1/e of its initial value; the solid line is a power law with exponent of  $-1/2$ ; the dashed curves indicate DW time scales for rearrangements ( $\tau_0$ ) and shear ( $\tau_s$ ).

higher than about  $3 \cdot 10^4$  /s, the stress relaxation is essentially exponential and the two relaxation times are hence indistinguishable. In this regime, shear completely dominates the relaxation. It is puzzling that the relaxation time decreases with increasing strain rate as  $\dot{\gamma}^{-1/2}$ , since on dimensional grounds one would have expected  $\dot{\gamma}^{-1}$ .

Now we may compare the macroscopic rheology with the nature of the microscopic bubble dynamics. Previously we used DW to measure the strain rate dependence of two microscopic time scales:  $\tau_0$ , the time between localized discrete rearrangements, and  $\tau_s$ , the time for adjacent scattering sites to convect apart by one wavelength of light [13]. The observed DW data are reproduced by the dashed curves in Fig. 3 (b). For very low strain rates, below about  $3 \cdot 10^4$  /s, the rearrangements are discrete and the time between events,  $\tau_0$ , is not noticeably different from the quiescent value. The stress relaxation time is much much longer than  $\tau_0$  - in-

dicating that the cooperative effect of many coarsening-induced rearrangements is required. For slightly higher rates, the time between events decreases, roughly as  $\dot{\gamma}^{-1/2}$ , just like the stress relaxation time. Since the stress relaxation time is now shorter than  $\tau_0$ , not every site in the foam must rearrange in order to relax the overall stress. Shear-induced events begin to dominate over coarsening-induced events at strain rates near  $\dot{\gamma}_c = \dot{\gamma}_{oq} = 0.025/s$ , where  $\dot{\gamma}_y = 0.05$  is the yield strain. At still higher rates, events merge together and the flow becomes progressively more homogeneous and smooth. The crossover strain rate is  $\dot{\gamma}_m = \dot{\gamma}_d = 0.5/s$ , where  $\tau_d = 0.1$  s is the duration of rearrangements [13]. Many physical quantities display a change in character above and below  $\dot{\gamma}_m$  [23]. Indeed, just below  $\dot{\gamma}_m$ , the new rheological measures of elasticity vanish at precisely where we no longer can detect discrete rearrangements (i.e. at the endpoint of the dashed curve for  $\tau_0$ ). At higher strain rates, the bubble motion is dominated entirely by uniform shear, as characterized by the DW S time scale  $\tau_s$ . The onset of this correlated shearing motion of bubbles (i.e. the starting point of the  $\tau_s$  curve) corresponds quite well to where  $G(\dot{\gamma}; \tau)$  begins to drop.

Finally, we note that the dramatic changes in the elastic character of the foam with strain rate are not reflected very strongly in the viscosity of the foam. As seen in Fig. 3(c), the viscosity decreases across the whole strain rate range, though not quite as fast as  $\dot{\gamma}^{-1}$  (which would have indicated constant stress). There is at most a slight change in exponent at  $\dot{\gamma}_m$ . Similar behavior is found in simulations [24]. Altogether this emphasizes the importance of the superposition method to measure  $G(\dot{\gamma}; \tau)$ , since it provides a clear dramatic signature of the unjamming transition. With this tool, and by comparison with DW S data, we have succeeded in connecting the nature of microscopic bubble dynamics with the resulting macroscopic rheological behavior. We have thereby shown that the unjamming of foam can be accomplished both by time and by application of shear. The unjammed liquid-like state is very similar to what would be achieved by raising the temperature for a thermal system. An important next step would be to deduce an effective temperature, recently shown in simulation of a sheared model foam to have many of the attributes of a true statistical mechanical temperature [25].

We thank A. J. Liu and P. T. Mather for helpful discussions. This work was supported by NASA Microgravity Fluid Physics grant NAG 3-2481.

- 
- [1] R. K. Prud'homme and S. A. Khan, *Foam: Theory, Measurement, and Applications*, vol. 57 of *Surfactant Science Series* (Marcel Dekker, New York, 1996).
  - [2] D. Weaire and S. Hutzler, *The Physics of Foams* (Oxford University Press, New York, 1999).
  - [3] H. M. Princen, *J. Coll. I. Sci.* 91, 160 (1983).
  - [4] T. G. Mason, J. Bibette, and D. A. Weitz, *Phys. Rev. Lett.* 75, 2501 (1995).
  - [5] A. Saint-Jalmes and D. J. Durian, *J. Rheol.* 43, 1411 (1999).
  - [6] A. J. Liu and S. R. Nagel, eds., *Jamming and Rheology* (Taylor and Francis, New York, 2001).
  - [7] A. J. Liu and S. R. Nagel, *Nature* 396, 21 (1998).
  - [8] D. J. Durian, D. J. Pine, and D. A. Weitz, *Science* 252, 686 (1991).
  - [9] A. D. Gopal and D. J. Durian, *J. Opt. Soc. Am.* 14, 150 (1997).
  - [10] S. Cohen-Addad and R. Hohler, *Phys. Rev. Lett.* 86, 4700 (2001).
  - [11] J. C. Eamshaw and A. H. Jafaar, *Phys. Rev. E* 49, 5408 (1994).
  - [12] A. D. Gopal and D. J. Durian, *Phys. Rev. Lett.* 75, 2610 (1995).
  - [13] A. D. Gopal and D. J. Durian, *J. Coll. I. Sci.* 213, 169 (1999).
  - [14] J. D. Ferry, *Viscoelastic Properties of Polymers* (Wiley, New York, 1980), 3rd ed.
  - [15] C. W. Macosko, *Rheology Principles, Measurements, and Applications* (VCH Publishers, New York, 1994).
  - [16] S. A. Khan, A. Schnepper, and R. C. Armstrong, *J. Rheol.* 31, 69 (1988).
  - [17] S. Cohen-Addad, H. H. Oballah, and R. Hohler, *Phys. Rev. E* 57, 6897 (1998).
  - [18] D. M. A. Buzza, C.-Y. D. Lu, and M. E. Cates, *J. Phys. II France* 5, 37 (1995).
  - [19] A. J. Liu, S. Ramaswamy, T. G. Mason, and D. A. Weitz, *Phys. Rev. Lett.* 76, 3017 (1996).
  - [20] D. J. Durian, D. A. Weitz, and D. J. Pine, *Science (USA)* 252, 686 (1991).
  - [21] H. C. Booij, *Rheol. Acta* 5, 222 (1966).
  - [22] I. K. Ono, Ph.D. thesis, University of California at Los Angeles (2002).
  - [23] I. K. Ono, S. Tewari, S. A. Langer, and A. J. Liu, submitted to *Phys. Rev. E* (2002).
  - [24] S. A. Langer and A. J. Liu, *Europhys. Lett.* 49, 68 (2000).
  - [25] I. K. Ono, C. S. O'Hern, D. J. Durian, S. A. Langer, A. J. Liu, and S. R. Nagel, to appear in *Phys. Rev. Lett.* (2002).